Journal of Alloys and Compounds 505 (2010) 96–100

Contents lists available at ScienceDirect

Journal of Alloys and Compounds

journal homepage: www.elsevier.com/locate/jallcom

Effects of a high magnetic field on the coarsening of MnBi grains solidified from isothermal annealed semi-solid melt

Changsheng Lou[a,b], Qiang Wang[a,*], Tie Liu[a], Ning Wei[a], Chunjiang Wang[a], Jicheng He[a]

[a] Key Laboratory of Electromagnetic Processing of Materials (Ministry of Education), Northeastern University, Shenyang 110004, Liaoning, People's Republic of China
[b] School of Materials Science and Engineering, Shenyang Ligong University, Shenyang 110168, People's Republic of China

ARTICLE INFO

Article history:
Received 24 February 2010
Received in revised form 7 June 2010
Accepted 9 June 2010
Available online 18 June 2010

Keywords:
Intermetallics
Coarsening
Texture
Semi-solid processing
High magnetic fields

ABSTRACT

With the imposition of a high magnetic field up to 11.5 T, the morphologic transition of the MnBi phase and the magnetic properties of the Bi–4.36 wt.% and 8.25 wt.% Mn alloy specimens solidified from a semi-solid state were investigated. Compared with the irregular shape and unequal dimensions of MnBi grains under 0 T, the coarsened MnBi grains were connected together and tended to be parallel to the direction of the external field of 11.5 T. The changes might be attributed to the Ostwald ripening of ferromagnetic grains in the isothermal holding stage and subsequent aggregation along the direction of external field driven by mutual magnetic force among the grains. The uniform orientation of the ferromagnetic MnBi grains obtained in the microstructures effectively improves the saturation magnetization of the Bi/MnBi composite materials, but the oversized grains and the defects in grains make the coercivity decrease.

1. Introduction

The application of high magnetic fields (HMFs) has drawn great attention in the material science, especially in the solidification and the annealing processes of alloys. One of the obvious results is the crystallographically aligned microstructure occurred with the imposition of an external field even for paramagnetic and diamagnetic materials [1–6]. It was recognized that the imposition of a high magnetic field during solidification of alloys would limit vigorous convection. Furthermore, during the solidification of dendrite grains in the melt, semi-solid region plays a key role in solidified microstructure because of a number of processes taking place simultaneously within this stage, such as crystallization, solute redistribution, ripening, interdendritic flow and solid movement [7]. Therefore the evolution of the microstructure of solid phase during liquid/solid stage becomes a key factor in final structure and property of alloys solidified under a high magnetic field.

Usually, the Bi–Mn alloy is used as experimental alloy system under high magnetic field conditions because it is a unique system for investigating the effect of microstructure changes induced by solidification on physical properties [8–12]. Just as shown in several works of research [10–12], ferromagnetic MnBi grains align regularly along the magnetic field in Bi–(0.9–10)wt.% Mn alloy solidified in the 2.5–5 T magnetic fields, and the morphology of MnBi grains represents as small flake or aggregated rod-like shape. In this study, Bi–Mn alloys were partially re-melted and solidified under HMFs to investigate the effects of HMFs on the coarsening and coalescence of the MnBi phase in semi-solid state and further on the magnetic properties of the prepared Bi–Mn composite alloy.

2. Experimental procedure

Raw materials were prepared by vacuum induction melting electrolytic Mn flakes and Bi particles with nominal content Bi–4 wt.% Mn and Bi–8 wt.% Mn and quenched to room temperature. The compositions of the two ingots were confirmed by chemical wetting analysis to be 4.36 wt.% Mn and 8.25 wt.% Mn, respectively. Cylindrical specimens of 10 mm in diameter and 15 mm in height were cut from the as-cast ingot. The experimental setup has been illustrated in a previous work [13]. Solidification experiments of the Bi–Mn alloys below liquidus temperature were undertaken with or without HMFs. The specimens were reheated to the temperature of 320 °C and kept for 30 min at this temperature. They were then cooled down to a temperature of 180 °C (lower than the eutectic temperature) at a cooling rate of 5 °C/min and finally to room temperature in the furnace. During the experiments, the flux density of uniform magnetic fields was 0 T and 11.5 T, respectively.

Specimens obtained from experiments were cut in half along the longitudinal axis. After conventional grinding and polishing, the microstructure examination was conducted using a Zeiss optical microscope. X-ray diffraction (XRD) analysis was carried out using a D/MAX 2400 diffractometer with Cu Kα radiation to determine the phases and to analyze the orientations of the MnBi crystals. The texture of the MnBi phase in solidified structures was examined by using X-Pert Pro diffractometer with Co radiation. The magnetic properties of the specimens were measured by using a vibrating sample magnetometer.

* Corresponding author. Tel.: +86 24 83681726; fax: +86 24 83681758.
E-mail address: wangq@epm.neu.edu.cn (Q. Wang).

0925-8388/$ – see front matter © 2010 Elsevier B.V. All rights reserved.
doi:10.1016/j.jallcom.2010.06.050

3. Results and discussion

3.1. Effects of HMFs on the morphology transition and alignment of the MnBi grains

Fig. 1 shows the microstructures of the Bi–Mn alloys solidified under various conditions. Fig. 1(a) and (c) represents the structure of the Bi–4.36 wt.% Mn and Bi–8.25 wt.% Mn solidified under 0 T, respectively. As it can be seen, the darker grains corresponding to MnBi phases are distributed randomly in Bi/MnBi eutectic matrix, and grains were characterized by their irregular shapes and unequal dimensions. In contrast to this case, the morphology of MnBi grains in structures solidified under an 11.5 T magnetic field (Fig. 1(b) and (d)) showed great differences. Firstly, MnBi grains coarsened with bigger dimensions and the shape of tip changed to be round. Secondly, the coarsened grains became elongated and formed long "touching" chains. Finally, the long axis of grains tended to be parallel to the direction of the imposed field. High magnification microstructures were examined to study the interplay among grains, as shown in Fig. 2. The grain boundaries in "touching" chains were denoted by white dot lines. Many liquid drops (i.e. Bi phase) were observed in the specimens solidified under 0 T (Fig. 2(a) and (c)); whereas less liquid drops appeared in the elongated coarsen MnBi grains with the imposed HMFs (Fig. 2(b) and (d)). These results imply that the HMFs playing roles on the morphological transition is not only in the growth stage, but also in the coarsening process which occurred in the thermal holding stage.

Generally, grains are uniform and coarsen in the solidified structures from a semi-solid process. Semi-solid grain coarsening is a two-phase coarsening process. LSW theory, developed independently by Lifshitz and Slyozov [14], and Wagner [15], is the classical theory for coarsening of a low volume fraction, dispersed second phase, and it is applicable to the solid/liquid system too. The driving force for coarsening in the solid/liquid two-phase systems is the reduction in interfacial free energy when the coarsening of solid grains results in an overall decrease in solid/liquid interfacial area. In this study, at the 11.5 T field, the grains coarsened in the direction perpendicular to the field and elongated in the direction parallel to the field. Since LSW theory cannot explain the above results completely, grain growth should be affected by others factors.

One reason of the formation of the coarsened MnBi grains in final structure is the Ostwald ripening, in which isolated particles grow at the expense of smaller particles [16] during semi-solid state. Another one should be attributed to the interaction among the magnetized MnBi grains at same time which result in the "touching" chains merging of larger particles by coalescence [17].

Grain growth velocity is controlled by the solute concentration gradient in the front of the solid/liquid interface, thus the MnBi phase growth in different direction is determined by the Mn content around the unmelted solid MnBi grains in the semi-solid stage. Because the easy magnetization *c* axis of the magnetized MnBi grains is parallel to the direction of the magnetic field during semi-solid stage, it results from the reorientation of these solid ferromagnetic grains induced by magnetic moment [1]. Therefore, the local inductive magnetic field around grains changed. So the solute concentration field around the unmelted big grain is no longer uniform under the case of the HMF application, but it is determined by the local inductive field of the magnetized MnBi grains. Yasuda et al. have interpreted the formation mechanism of aligned MnBi grains in annealed Bi–Mn alloy [18]. Since the magnetic field induced by magnetization of a MnBi grain is the highest at the magnetic pole, free energy near the pole is the minimum. Thus, the magnetization energy has influences on phase equilibrium. As a result, the Mn concentration in liquid near the pole becomes lower than that

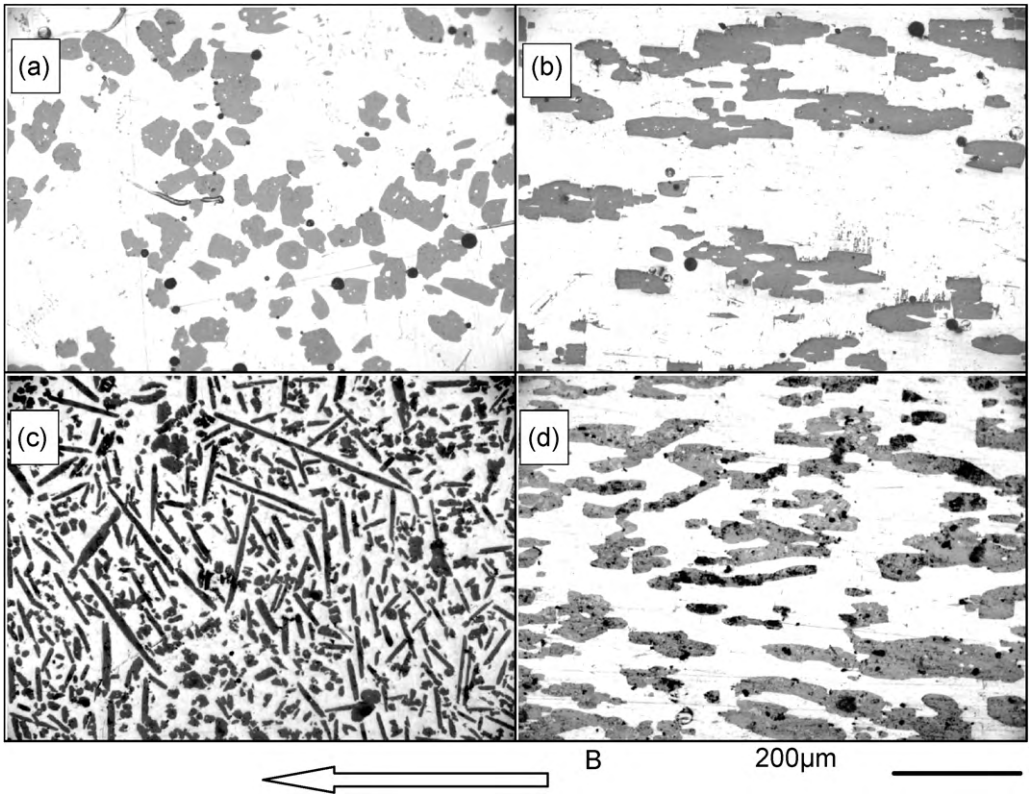

Fig. 1. Typical microstructures of Bi–Mn alloys solidified under various conditions: (a) Bi–4.36 wt.% Mn at 0 T; (b) Bi–4.36 wt.% Mn at 11.5 T; (c) Bi–8.25 wt.% Mn at 0 T; (d) Bi–8.25 wt.% Mn at 11.5 T. The arrowhead indicates the direction of the imposed field.

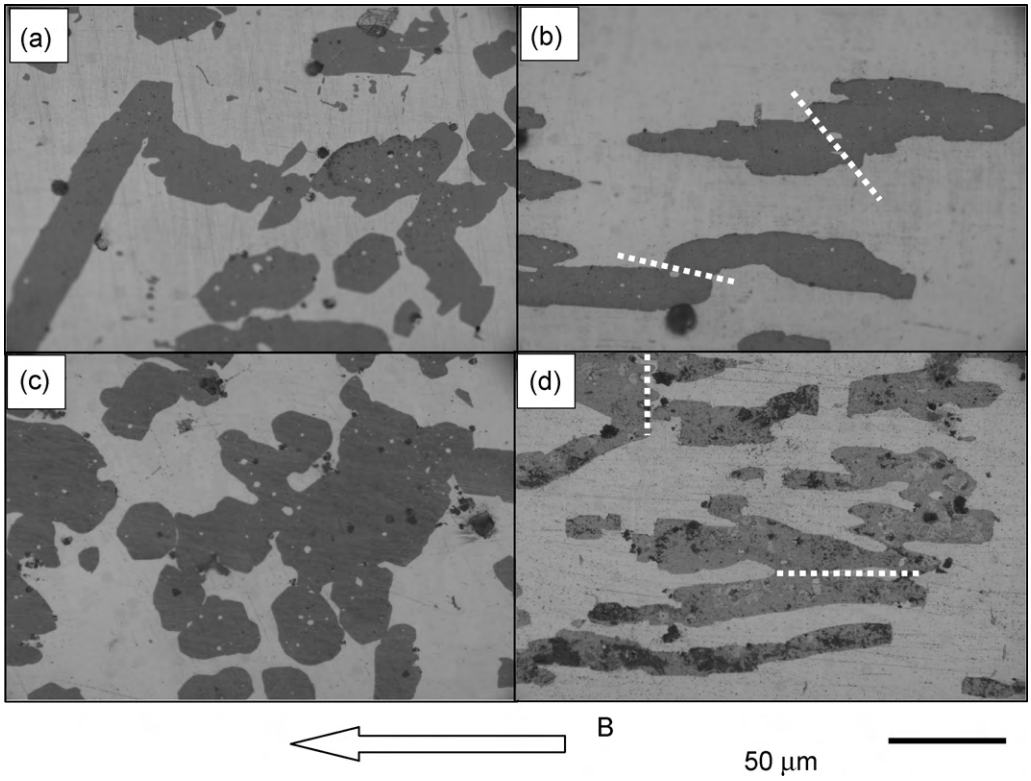

Fig. 2. Typical microstructures of Bi–Mn alloys solidified under various conditions, high magnification: (a) Bi–4.36 wt.% Mn at 0 T; (b) Bi–4.36 wt.% Mn at 11.5 T; (c) Bi–8.25 wt.% Mn at 0 T; (d) Bi–8.25 wt.% Mn at 11.5 T. The arrowhead indicates the direction of the imposed field.

in other regions. The Mn concentration difference induced by the magnetic field promotes the diffusion of Mn atoms to the pole. This model describes the case of a semi-solid stage. The schematic illustrations of solute concentration around unmelted ferromagnetic MnBi grain with and without the imposed HMF are shown in Fig. 3. Without imposition of high magnetic field, the solute concentration decreases from the solid/liquid interface to far uniformly in all directions, while most of the Mn atoms are attracted to the magnetic pole under a high magnetic field, therefore local concentration is higher than the average level in melt. The solute content may enhance the growth velocity in the direction of magnetic axis and results in formation of the elongated grains.

In addition to the above interplay between the magnetized grains and the imposed field on the growth of MnBi grains, interactions among magnetized grains also play an important role in the morphological transition. When the distance between two magnetic poles reaches critical range, grains connect each other to forming chains under the effect of attracting force, which is expressed as $F_a = M_1 M_2 \cos\alpha/(4\pi\mu d^2)$ [19], where M_1, M_2 are magnetic moment of two isolated grains, α is the angle and d is the spacing between two vectors M_1, M_2. The morphological transition is influenced by the combined action of the above effects of HMF.

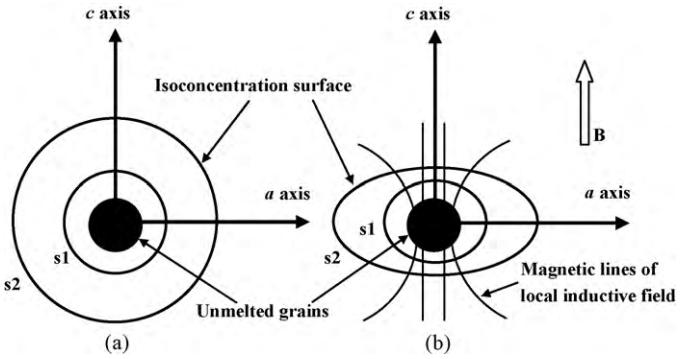

Fig. 3. Schematic profile of solute concentration around MnBi grain in the ripening stage at (a) 0 T and (b) 11.5 T. s1 and s2 denote the solute isoconcentration around MnBi grains. "*a* axis" and "*c* axis" represent the crystallographic axes of MnBi grain, respectively.

Therefore, the coarsening and coalescence of the MnBi grains result from the ripening process of isolated particles, interaction among magnetized grains, and the anisotropic growth of the MnBi grains during semi-solid stage. Meanwhile, the effect of subsequent growth of the MnBi grains on alignment of "touching" chains cannot be ignored.

As seen in Fig. 1(c) and (d), the long axis of MnBi grains tend to be parallel to the direction of the imposed field with different degree of deviation for Bi–4.36 wt.% Mn and Bi–8.25 wt.% Mn alloys. The statistical analysis of misorientation between the long axis and the field direction was obtained by quantitative metallographic analysis method and the results are shown in Fig. 4. Most misorientation is less than 10° in Bi–4.36 wt.% Mn alloy; whereas several misorientation even may reach about 30° in Bi–8.25 wt.% Mn alloy. The known mechanism of particle rotation on the particle aspect ratio in melt cannot completely explain the results, which should be attributed to the difference of the solid volume in melt. According to Lever law, the volume fractions of unmelted MnBi phase at 320 °C in experimental alloys are 11.3% (Bi–4.36 wt.% Mn) and 16.8% (Bi–8.25 wt.% Mn). For Bi–8.25 wt.% Mn alloy in this study, the relatively higher volume fraction hindered the rotation of grains in melt. Simultaneously, the spacing among solid MnBi grains in Bi–8.25 wt.% Mn alloy melt is lower than that in Bi–4.36 wt.% Mn alloy melt, so the correspondent interaction among grains was much larger than that in Bi–4.36 wt.% Mn alloy melt. The previously mentioned solute concentration change and interaction between magnetized MnBi grains can successfully explain the morphological transition.

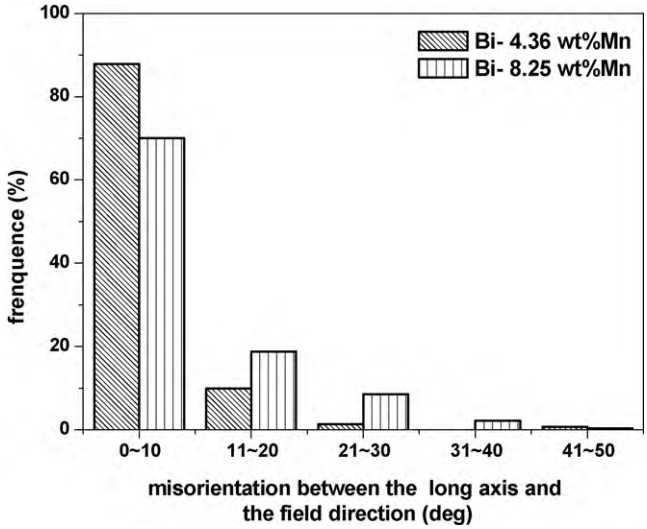

Fig. 4. Statistical analysis of the misorientation between the long axis of MnBi grains and the direction of the imposed field.

3.2. Effect of HMFs on the orientation of the MnBi crystals

XRD analysis was conducted to determine the orientations of the MnBi crystals in specimens solidified under various conditions, as shown in Fig. 5. The pattern of Bi–8.25 wt.% Mn alloy was similar to that of Bi–4.36 wt.% Mn alloy at 0 T, in which almost all the peaks of the MnBi phase appeared, whereas only the (1 0 0), (1 1 0), (2 0 0) and (3 0 0) peaks were observed in specimens prepared under HMFs, and the (1 1 0) peak was the strongest in all the peaks observed. As the MnBi compound has a hexagonal NiAs type structure and its *c* axis is parallel to the direction of magnetic field, (1 1 0) plane becomes the strongest diffraction peak in the XRD patterns of the Bi–Mn alloys solidified under HMFs. Furthermore, the ⟨0 0 1⟩ inverse pole figures of Bi–4.36 wt.% Mn alloy in magnetic field direction are shown in Fig. 6. The crystallographic preferred orientation is more obvious at 11.5 T than that of at 0 T. The above results certify that the easy magnetization *c* axis of MnBi is parallel to the direction of the fields which resulted from the rotation of easy *c* axis of the MnBi phase and subsequent rapid growth along *c* axis.

Similar to the aligned structures of coarsened MnBi grains in Bi matrix, Shimotomai [20] and Zhang [21] found that the elongated ferrite grain microstructure occurred in Fe–C alloys during the austenitic transformation with application of a high magnetic

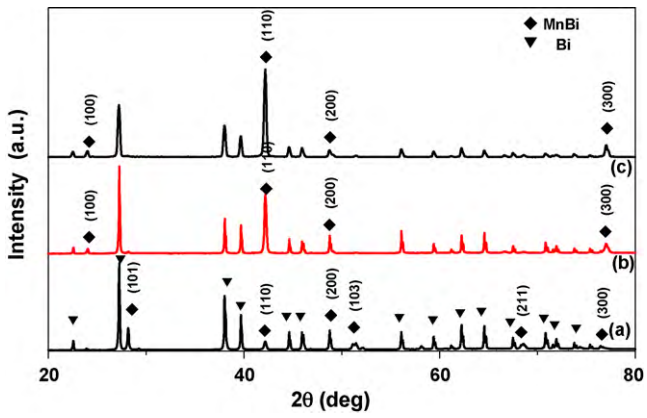

Fig. 5. XRD patterns of Bi–Mn alloys solidified under various conditions: (a) Bi–4.36 wt.% Mn alloy at 0 T; (b) Bi–4.36 wt.% Mn alloy at 11.5 T; (c) Bi–8.25 wt.% Mn alloy at 11.5 T.

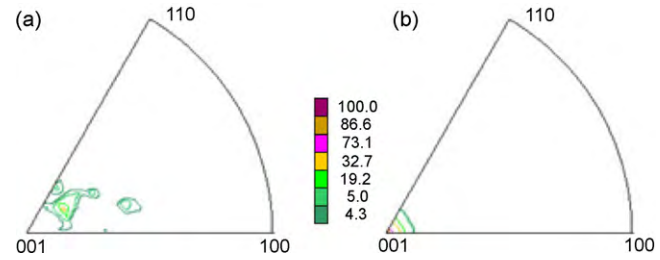

Fig. 6. ⟨0 0 1⟩ inverse pole figures of Bi–4.36 wt.% Mn alloy at (a) 0 T and (b) 11.5 T.

field, moreover they hold that it is the result of a balance of the magnetostatic and the interfacial energies.

3.3. Magnetic properties of the partial-melt Bi–Mn alloy solidified under HMFs

Fig. 7 shows the hysteresis loops of Bi–4.36 wt.% Mn alloy in the vertical and parallel directions, in which the obvious magnetic anisotropy of specimen solidified from partial-melt state under 11.5 T field was observed, which is attributed to the easy magnetization *c* axis parallel to the external field. The measured saturation magnetization is 5.63 emu/g along the parallel direction. MnBi crystal structure is NiAs type and its saturation magnetization moment is $3.9\mu_B$, so the single crystal saturation magnetization is 254 emu/cm^3 (29.5 emu/g). The measured value is close to the calculated value (6.28 emu/g) according to the MnBi volume fraction in Bi–4.36 wt.% Mn alloy, whereas the measured coercivity is 0.27 kOe only, far lower than theoretical value. So the probable influential parameter should be investigated.

The influential parameters on the coercivity of composite magnetic materials include the size of magnetic phase, numbers of domain in one grain and structural defects like dislocation, bumps and sharp corners. As seen from microstructures in Fig. 2(b) and (d), the big "touching" MnBi chains consist of several small grains, and more defects are in the boundaries, which go against the coercivity. Moreover, the defects in grains increase the number of nuclei of reversed domain. The existence of defects in boundaries reduces the coercivity in this study, too. Therefore the oversized grains and the defects in "touching" grains decrease the coercivity of prepared Bi–Mn alloy.

As shown in Fig. 7, the saturation magnetization is close to the theoretical value, whereas the coercivity greatly differs from theoretical value. The study indicates that partial-melt alloys solid-

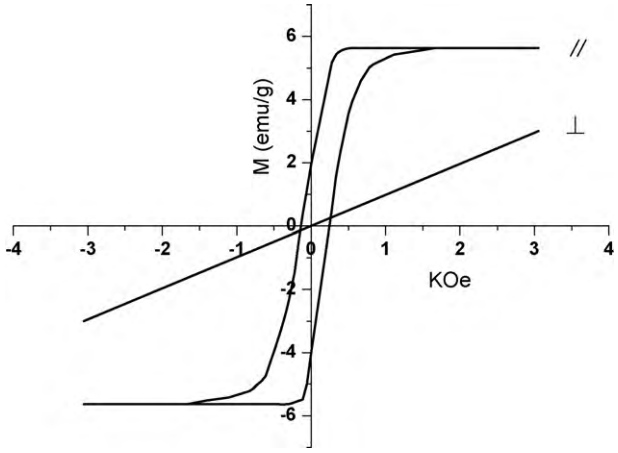

Fig. 7. Hysteresis loops of Bi–4.36 wt.% Mn alloy solidified from partial-melt state, the symbols //and ⊥ represents the directions perpendicular and parallel to imposed field.

ification under HMFs provides an opportunity for preparation for perfect composite magnets.

4. Conclusions

(1) Compared with the specimen solidified under 0 T, the grains are coarsened and connected together in those semi-solidified structures under HMFs. The morphological transition of MnBi grains resulting from the Ostwald ripening of ferromagnetic grains occurred in the isothermal holding stage during semi-solid process and the aggregation along the direction of external field driven by mutual magnetic force among grains.
(2) The long axis of MnBi grains and the direction of external field are not identical, especially in Bi–8.25 wt.% Mn alloy, due to the hindrance of grains rotation induced by higher volume fraction of solid particles in melt. But the easy magnetization *c* axis is parallel to the direction of external field, which is attributed to grains growth impacted in the liquid/solid coexistence stage and subsequent growth stage.
(3) The uniform orientation and the big size of ferromagnetic MnBi grains in the specimens solidified from semi-solid state effectively improve the saturation magnetization of composite materials, but the oversized grains and the defects in grains make the coercivity decrease seriously.

Acknowledgements

This work was financially supported by the Fundamental Research Funds for the Central Universities (grant nos. N090109001 and N090209001), the Program for New Century Excellent Talents in University (grant no. NCET-06-0289) and the 111 project (grant no. B07015).

References

[1] P. de Rango, M. Lees, P. Lejay, A. Sulpice, R. Tournier, M. Ingold, P. Germi, M. Pernet, Nature 28 (1991) 770–772.
[2] Y.D. Zhang, N. Gey, C.S. He, X. Zhao, L. Zuo, C. Esling, Acta Mater. 52 (2004) 3467–3474.
[3] T. Liu, Q. Wang, A. Gao, C. Zhang, C. Wang, J. He, Scripta Mater. 57 (2007) 992–995.
[4] Q. Wang, C. Lou, T. Liu, N. Wei, C. Wang, J. He, J. Phys. D: Appl. Phys. 42 (2009) 025001–025005.
[5] D.A. Molodov, S. Bhaumik, X. Molodova, G. Gottstein, Scripta Mater. 54 (2006) 2161–2164.
[6] H. Yasuda, K. Tokieda, I. Ohnaka, Mater. Trans. JIM 41 (2000) 1005–1021.
[7] C. Metron, Flemings, Metall. Trans. A 22 (1991) 957–981.
[8] M.N. Shetty, D.K. Rawat, K.N. Rai, J. Mater. Sci. 22 (1987) 1908–1912.
[9] K.Y. Ko, S.J. Choi, S.K. Yoon, Y.S. Kwon, J. Magn. Magn. Mater. 310 (2007) e887–889.
[10] E.M. Savitsky, R.S. Torchinova, S.A. Turanov, J. Cryst. Growth 52 (1981) 519–523.
[11] H. Yasuda, I. Ohnaka, Y. Yamamoto, A. Wismogroho, N. Takezawa, K. Kishio, Mater. Trans. JIM 44 (2003) 2550–2554.
[12] X. Li, Z.M. Ren, Y. Fautrelle, Intermetallics 15 (2007) 845–855.
[13] Q. Wang, T. Liu, A. Gao, C. Zhang, C.J. Wang, J.C. He, Scripta Mater. 56 (2007) 1087–1090.
[14] I.M. Lifshitz, V.V. Slyozov, J. Phys. Chem. Solids 19 (1961) 35–50.
[15] C. Wagner, Zeitschrift für Elektrochemie 65 (1961) 581–591.
[16] P.W. Voorhees, Annu. Rev. Mater. Sci. 22 (1992) 197–215.
[17] J.A. Warren, B.T. Murray, Model. Simul. Mater. Sci. Eng. 4 (1996) 215–229.
[18] H. Yasuda, A. Nakahira, I. Ohnaka, Y. Yamamoto, K. Kishio, Mater. Trans. JIM 44 (2003) 2555–2562.
[19] D.F. Wan, S.H. Luo, Physics of Magnetism, Electronic Industry Press, Beijing, 1987, p. 22.
[20] M. Shimotomai, K. Maruta, K. Mine, M. Matsui, Acta Mater. 51 (2003) 2921–2932.
[21] Y.D. Zhang, C. Esling, J. Muller, C.S. He, X. Zhao, L. Zuo, Appl. Phys. Lett. 87 (2005) 212504–212513.